Confocal light scattering spectroscopic imaging system for *in situ* tissue characterization

Peter Huang,[1,2] Martin Hunter,[1] and Irene Georgakoudi[1,*]

[1]Department of Biomedical Engineering, Tufts University, 4 Colby Street, Medford, Massachusetts 02155, USA

[2]Department of Mechanical Engineering, Binghamton University, Binghamton, New York 13902, USA

*Corresponding author: Irene.Georgakoudi@tufts.edu

Received 14 November 2008; revised 28 March 2009; accepted 3 April 2009; posted 9 April 2009 (Doc. ID 104120); published 29 April 2009

We report on the design and construction of a confocal light scattering spectroscopic imaging system aimed ultimately to conduct depth-resolved characterization of biological tissues. The confocal sectioning ability of the system is demonstrated using a two-layer sample consisting of a 200 μm thick cancer cell layer on top of a scattering layer doped with a green absorber. The measurement results demonstrate that distinct light scattering signals can be isolated from each layer with an axial and a lateral resolution of 30 and 27 μm, respectively. Such a system is expected to have significant applications in the areas of tissue engineering and disease diagnostics and monitoring. © 2009 Optical Society of America

OCIS codes: 170.6510, 180.1790, 290.1350, 290.5885, 300.6550.

1. Introduction

Light scattering properties of substances have been widely used to characterize and differentiate materials and their compositions, exploiting the fact that the intensity, angular distribution, and wavelength responses of light scattering depend on the size and refractive index of the scatterer and its constituents [1]. In biology and medicine, light scattering spectroscopy has been previously reported to be capable of providing spectral characteristics for identifying and distinguishing different cell types [2–6]. The usefulness of cellular light scattering has been further demonstrated when combined with flow cytometry [7] or microscopy [8,9].

While the most common method to examine cellular light scattering properties is through either forward [7,9] or side scattering [8], such measurement design is severely restricted in its applicability, especially for *in vivo* biomedical applications where forward and side scattering data collection geometries are practically impossible. This leaves backscattering as a very attractive option for collecting light scattering signals from cells and tissues *in vivo*. Previous studies have shown that backscattering signals from biological specimens can provide strong enough signals for cell characterization [2–5]. Recently, backscattering spectroscopy has been demonstrated to be capable of extracting the physical characteristics of scattering samples suspended in liquid medium [10], while Itzkan *et al.* [11] developed a confocal light absorption and scattering spectroscopic microscope to monitor organelles in living cells.

Most of the reported backscattering spectroscopic microscopy techniques are limited to measuring scattering characteristics of a single cell layer or the superficial tissue without any depth-sectioning ability. The ability to isolate morphological changes from a distinct depth could be of great clinical interest. For instance, in epithelial cancer, premalignant changes typically originate within layers of tissue buried under the surface; therefore the ability to detect morphological changes of underlying layers can contribute significantly to early cancer detection. In tissue engineering, depth-resolved light scattering measurements could provide dynamically highly sensitive and quantitative information with regards to important biomaterial properties, such as matrix remodeling and mineralization. To observe

0003-6935/09/132595-05$15.00/0

backscattering signals of living tissue specimens with optical sectioning ability, we designed and constructed a confocal light scattering spectroscopic microscope (CLSSM) system [shown in Fig. 1(a)].

There are a number of other reported optical techniques that can provide depth-resolved scattering information of biological tissues, including low-coherence enhanced backscattering spectroscopy [12], optical coherence tomography (OCT) [13], angle-resolved low-coherence interferometry [14], and confocal light absorption and scattering spectroscopic microscopy (CLASS) [11]. While low-coherence enhanced backscattering spectroscopy has shown exquisite sensitivity to cellular organization features, its optical penetration depth is limited to the most superficial 100 μm. OCT is a commonly used backscattering technique that also provides depth-resolved imaging of epithelial tissues, but its illumination bandwidth is typically limited to less than 100 nm, which is usually too narrow for investigating light scattering spectral characteristics of biological tissues. The angle-resolved low-coherence interferometry method focuses on using the angular characteristics of light scattering to extract specimen properties but does not exploit any wavelength spectral dependence. Still, simultaneous measurement of angular and spectral responses may provide better sample characterization capabilities than either measurement alone.

In contrast to the previously mentioned systems, the design of our system is relatively similar to that of the CLASS microscope, which has an axial resolution of 3 μm and has been used to isolate subcellular features as specimens are scanned in the lateral direction. However, the system described in this article is capable of performing depth-resolved

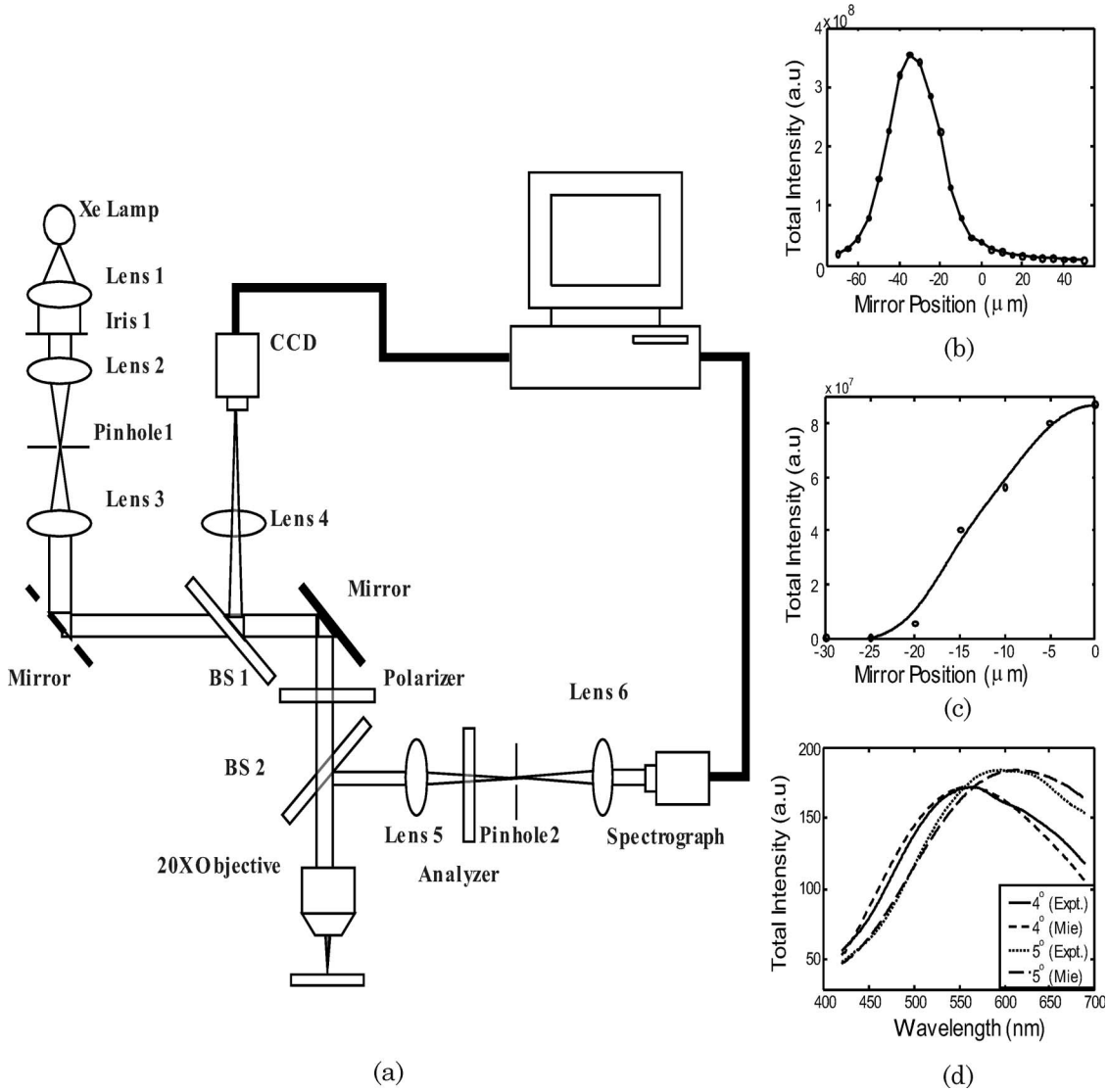

Fig. 1. (a) Schematic of the CLSSM. (b) Confocal axial resolution measurement of the CLSSM system. The circular markers are experimental measurements, while the solid line is a fit to the data. (c) Lateral resolution measurement of the CLSSM system. The circular markers are experimental measurements while the solid line is a fit to the data. (d) Light scattering spectral characteristics of 5 μm beads at polar angles of 4° and 5°, measured under collimated illumination and compared with Mie theory predictions.

measurements of thick tissue specimens and has the capability to resolve not only the wavelength dependence but also the polar angular dependence of the scattered light. These novel features specific to our system allow us to identify the distinctive angular scattering characteristics of a sample and exclude signals in the exact backward direction that can be contaminated by specular reflections.

2. Optical System Design and Experimental Procedures

The detailed optical setup of our CLSSM system is shown in Fig. 1(a). The illumination source is a 500 W xenon lamp whose emitted light is spatially filtered and collimated. The collimated white light is directed through a linear polarizer into a long-working-distance, infinity-corrected 20× microscope objective (Olympus). By doing so, the light beam emerges from the objective as a converging beam and focuses down onto a sample located at the front focal plane of the microscope objective, with an effective illumination numerical aperture of 0.30. Images of the sample are projected onto a CCD video camera through the microscope objective and a tube lens (lens 4) to provide visual confirmation of proper sample placement. Because the sample is placed at the front focal plane of the objective, scattered light off the sample forms an angular map on the Fourier plane located at the back focal plane (BFP) of the objective. This map is relayed to the entrance slit of a spectrograph (Oriel MS 127i, custom grating at 300 lines/mm blazed at 500 nm) through strategic placements of lenses 5 and 6 to form a telescope combination. As the 20× objective is infinity-corrected, lens 5 also simultaneously functions as a tube lens whose back focal plane is confocal to the sample plane. Therefore, we can reduce the contribution of scattered light from out-of-focus objects by placing a 200 μm pinhole at the back focal plane of lens 5 to achieve confocal sectioning. Since scattered light from the sample must pass through pinhole 2 to reach the entrance slit of the spectrograph, we essentially have a confocal light scattering spectroscopic microscope. To take advantage of scattering information that can be obtained through polarization analysis, an analyzer is inserted between lens 5 and pinhole 2, and the polarizer–analyzer combination in the system can be oriented to create either parallel or perpendicular polarization. In our image analysis, the scattering azimuthal angle is defined as the angle between the imaging slit and the plane of the illumination polarization, while the scattering polar angle is defined as the angle between the scattering direction and the exact backward direction of the illumination beam optical axis.

To measure the optical sectioning resolution of the CLSSM system, a surface-reflective mirror was used as a sample scatterer and the intensity of the reflected light passing through the confocal pinhole was obtained at various axial mirror positions. The optical sectioning resolution was then defined as the full width at half-maximum of the collected intensity profile. As shown in Fig. 1(b), the optical sectioning resolution of our system is 30 μm. In contrast to the system reported by Itzkan *et al.* [11], whose aim was to observe intracellular light scattering with its 3 μm axial resolution, our CLSSM system's larger axial resolution makes it more suitable for observing multicellular-level light scattering differences within a biological tissue of a few hundred micrometers in thickness. The lateral resolution of the CLSSM system was also measured by using the edge of a sharp blade as a sample scatterer, and was found to be 27 μm [Fig. 1(c)].

Proper alignment of the system was confirmed by collecting backscattering signals from 5 μm polystyrene microspheres under collimated illumination, created by a temporary placement of a convex lens between a beam splitter, BS1 [Fig. 1(a)], and the mirror that directs the illuminating light into the microscope object. This convex lens then focused the illuminating light beam onto the back focal plane of the objective to create collimated illumination onto the microsphere solution. Scattering signals from the microspheres were compared with Mie theory predictions for system validation. Optical alignment optimization was achieved when parallel mapping between image pixel positions and scattering polar angles was accomplished through a quantitative comparison of the spectral responses between the measurements and the simulation [as shown in Fig. 1(d)].

Cultured human cancerous cells of low passage number (<20) were used as biological samples to demonstrate the capabilities of the CLSSM. Specifically, leukemia (NALM-6) cells were cultured in a sterile environment in RPMI 1640 (88%), penicillin/streptomycin (1%), and fetal bovine serum (10%). The cells were passaged twice a week and were harvested and suspended in a clear medium (99% RPMI 1640, 1% penicillin/streptomycin) for imaging. Before imaging, the suspended NALM-6 cells were allowed to settle to the bottom of a cell chamber to simulate thick tissue layers.

3. Results and Discussion

The ability of our CLSSM system to provide confocal spectroscopic scattering analysis is demonstrated by collecting signals from an aggregate sample shown in Fig. 2. Multiple layers of NALM-6 cells yielding an overall thickness of approximately 200 μm were allowed to settle at the bottom of a cell chamber. Simultaneously, green food coloring was added to nondiluted dairy cream composed of fatty emulsion particles as diffuse scatterers and placed in another chamber to represent a highly scattering and absorbing medium. The spectral characteristics of the NALM-6 cells and the green scattering layer were individually captured using the CLSSM system (control experiments), and then the two samples were stacked on top of each other, separated by a coverslip as shown in Fig. 2. The backscattering signals of the

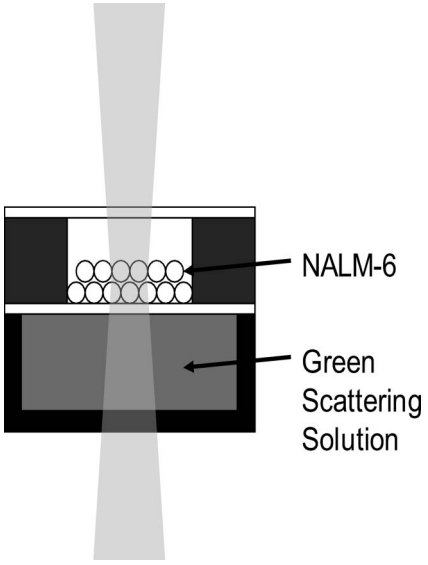

Fig. 2. Schematic of the layering of leukemia cancer cells (NALM-6) on top of a green scattering solution.

stacked NALM-6 cell layers and the green scattering solution were then collected to be compared with the stand-alone control group samples.

The spectral characteristics of all samples are shown in Fig. 3. When analyzing the images, we normalized the scattering maps based on the following formula:

$$I_{\text{norm}} = \frac{I_{\text{raw}} - I_{\text{BG}}}{I_{99\%}},$$

where I_{norm} is a normalized scattering intensity map, I_{raw} is the raw scattering map of a sample, I_{BG} is a raw image taken under the sample experimental condition in the absence of the sample, and $I_{99\%}$ is a spectral calibration curve of the system using a 99% reflection standard to eliminate the emission characteristics of the lamp and the spectral characteristics of the CCD pixel sensitivities. In Figure 3(a) the scattering polar angle versus wavelength map of the superficial NALM-6 cells on the top partition of the stacked sample is shown, while the same type of scattering map for the green scattering solution at 60 μm below the bottom surface of the partitioning glass coverslip (170 μm thick) is shown in Fig. 3(b). Both maps were taken at an azimuthal angle of 45° under parallel polarization. One can observe that in Figs. 3(a) and 3(b) there exists a bright region midway between the top and the bottom of each image (near scattering polar angle 0°). This is the result of the illuminating light's specular reflection off the glass coverslip that separates the NALM-6 cells from the green scattering solution. From these images, one can notice that the bright specular reflection regions extend from scattering polar angles of −3.5° to +3.5° , and therefore we always excluded this bright region in our image analysis.

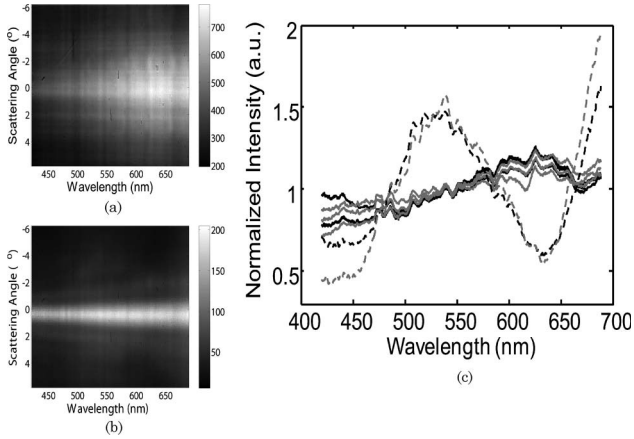

Fig. 3. (a) Scattering polar angle versus wavelength map of the NALM-6 cells on the top half of the aggregate sample shown in Fig. 2. (b) Scattering polar angle versus wavelength map of the green scattering layer on the bottom half of the aggregate sample shown in Fig. 2. (c) Spectral dependence of the integrated backscattering intensities for stand-alone control group samples and the stacked experimental group samples: NALM-6 cells alone (black solid line; control group), green scattering solution alone (black dashed line; control group), and the stacked NALM-6 (gray solid line; experimental group) and green scattering solution (gray dashed line; experimental).

Figure 3(c) presents the spectral dependence of integrated backscattering intensities for NALM-6 cells alone (black solid lines; multiple samplings, control group), green scattering solution alone (black dashed line: average response, control group), and the stacked NALM-6 (gray solid lines: multiple samplings) and green scattering solution (gray dashed line: average response). Specifically, scattering signals from the stacked green scattering solution was taken at 430 μm below the surface layer of the NALM-6 cells. The integrated backscattering intensity was defined as the sum of signal intensity within a polar angle of −4° and −6°. In Fig. 3(c), 3 data sets are shown for the NALM-6 samples, and each data set represents measurements obtained from one group of NALM-6 cells. This is because the NALM-6 cells, being a biologically living sample, have a higher probability of having group-to-group variability, and measurements of multiple groups were conducted to demonstrate repeatability. In contrast, only the average spectral dependency from three measurements is shown for the green scattering solution samples in Fig. 3(c) to enhance visibility of the salient features of the graph, since the signal from such sampled varied less than 3%.

In the stand alone control group samples, the NALM-6 cells are observed to have a trend of increasing intensity with increasing measurement wavelength [Fig. 3(c)]. The scattering signals of the emulsion particles in the green scattering solution, in contrast, are dominated by strong light absorption of the green dye in the blue/violet (<470 nm) and in the red wavelengths (580–650 nm), when compared with the signals from the NALM-6 cells. Thus, we anticipated that such spectral characteristics can be utilized to demonstrate the CLSSM system's confocal sectioning ability if we were able to make the same

observation with green scattering solutions placed underneath a thick NALM-6 cell multilayer. Indeed for the stacked samples both the NALM-6 cell layers on the top and the green scattering solution on the bottom show spectral characteristics similar to that of the respective stand-alone control samples in Fig. 3(c). That is, the backscattering spectral responses at a similar depth of the stacked NALM-6 cell layers closely resemble that of the stand-alone control NALM-6 samples, while the backscattering signals acquired from the green scattering emulsion particles on the bottom is dominated by the same green dye light absorption of the control samples. Therefore, results in Fig. 3(c) validate the confocal sectioning capability of our CLSSM system to collect light scattering signals originating from objects underneath a relatively thick layer of biological cells. It should again be noted that the agreement of scattering spectral profiles between the stacked and the stand-alone control samples was observed only for scattering polar angles greater than 3.5° from the exact backward direction, outside the bright region of specular reflections. The fact that we can capture the angle-specific scattering spectrum allows us to identify the extent of specular reflections and properly exclude such intensities in image analysis. Image data taken from a fiber-based system such as the CLASS reported by Itzkan *et al.* [11] contains all scattering intensities without angular discrimination and can be contaminated by specularly reflected light, which could in turn affect the accuracy and sensitivity of the approach.

4. Concluding Remarks

The data shown in Fig. 3 provides proof of our system's capacity to capture the unique scattering spectroscopic properties of different materials with confocal imaging capability. The optical sectioning ability of our CLSSM system to collect light scattering signals from scatterers buried under a 200 μm thick cell layer illustrates its potential as a noninvasive characterization tool for biological tissues that extend hundreds of micrometers. The approach allows exploitation of either or both of the wavelength and scattering-angle dependence of the backscattered light, which may allow for improved optimization depending on the nature of the sample and application. In addition, the scattering-angle resolution capabilities of the system allow for a fairly straightforward way to identify and eliminate specular or other spurious reflections, which could otherwise introduce artifacts. The CLSSM spectral imaging capabilities are expected to be particularly relevant to disease diagnostic applications that would benefit from sensitive detection of depth-resolved features, as in the case of early cancer screening. In addition, CLSSM may be a useful tool for tissue engineering applications, in terms of assessing dynamically key features, such as mineral deposition and extracellular matrix remodeling and organization.

The work presented in this paper was financially supported by the National Institute of Health through grant NIH (R21CA114684).

References

1. C. F. Bohren and D. R. Huffman, *Absorption and Scattering of Light by Small Particles* (Wiley, 1983).
2. C. Mujat, C. Greiner, A. Baldwin, J. M. Levitt, F. Tian, L. A. Stucenski, M. Hunter, Y. L. Kim, V. Backman, M. Feld, K. Munger, and I. Georgakoudi, "Endogenous optical biomarkers of normal and human papillomavirus immortalized epithelial cells," Int. J. Cancer **122**, 363–371 (2008).
3. V. Backman, V. Gopal, M. Kalashnikov, K. Badizadegan, R. Gurjar, A. Wax, I. Georgakoudi, M. Mueller, C. W. Boone, R. R. Dasari, and M. S. Feld, "Measuring cellular structure at submicrometer scale with light scattering spectroscopy," IEEE J. Sel. Top. Quantum Electron. **7**, 887–893 (2001).
4. G. Schuele, E. Vitkin, P. Huie, C. O'Connell-Rodwell, D. Palanker, and L. T. Perelman, "Optical spectroscopy noninvasively monitors response of organelles to cellular stress," J. Biomed. Opt. **10**, 051404 (2005).
5. C.-C. Yu, C. Lau, J. W. Tunnell, M. Hunter, M. Kalashnikov, C. Fang-Yen, S. F. Fulghum, K. Badizadegan, R. R. Dasari, and M. S. Feld, "Assessing epithelial cell nuclear morphology by using azimuthal light scattering spectroscopy," Opt. Lett. **31**, 3119–3121 (2006).
6. J. R. Mourant, T. M. Johnson, S. Carpenter, A. Guerra, T. Aida, and J. P. Freyer, "Polarized angular dependent spectroscopy of epithelial cells and epithelial cell nuclei to determine the size scale of scattering structures," J. Biomed. Opt. **7**, 378–387 (2002).
7. V. Ost, J. Neukammer, and H. Rinneberg, "Flow cytometric differentiation of erythrocytes and leukocytes in dilute whole blood by light scattering," Cytometry **32**, 191–197 (1998).
8. M. T. Valentine, A. K. Popp, D. A. Weitz, and P. D. Kaplan, "Microscope-based static light-scattering instrument," Opt. Lett. **26**, 890–892 (2001).
9. W. J. Cottrell, J. D. Wilson, and T. H. Foster, "Microscope enabling multimodality imaging, angle-resolved scattering, and scattering spectroscopy," Opt. Lett. **32**, 2348–2350 (2007).
10. Y. Liu, X. Li, Y. L. Kim, and V. Backman, "Elastic backscattering spectroscopic microscopy," Opt. Lett. **30**, 2445–2447 (2005).
11. I. Itzkan, L. Qiu, H. Fang, M. M. Zaman, E. Vitkin, I. C. Ghiran, S. Salahuddin, M. Modell, C. Andersson, L. M. Kimerer, P. B. Cipolloni, K.-H. Lim, S. D. Freedman, I. Bigio, B. P. Sachs, E. B. Hanlon, and L. T. Perelman, "Confocal light absorption and scattering spectroscopic microscopy monitors organelles in live cells with no exogenous labels," Proc. Natl. Acad. Sci. U.S.A. **104**, 17255–17260 (2007).
12. Y. L. Kim, Y. Liu, V. M. Turzhitsky, R. K. Wali, H. K. Roy, and V. Backman, "Depth-resolved low-coherence enhanced backscattering," Opt. Lett. **30**, 741–743 (2005).
13. J. M. Schmitt, "Optical coherence tomography (OCT): a review," IEEE J. Sel. Top. Quantum Electron. **5**, 1205–1215 (1999).
14. K. J. Chalut, S. Chen, J. D. Finan, M. G. Giacomelli, F. Guilak, K. W. Leong, and A. Wax, "Label-free, high-throughput measurements of dynamic changes in cell nuclei using angle-resolved low coherence interferometry," Biophys. J. **94**, 4948–4956 (2008).